JACS
JOURNAL OF THE AMERICAN CHEMICAL SOCIETY

pubs.acs.org/JACS

Communication

An S_{10}-Symmetric 5-Fold Interlocked [2]Catenane

Tanya K. Ronson, Yujia Wang, Kim Baldridge,* Jay S. Siegel,* and Jonathan R. Nitschke*

Cite This: *J. Am. Chem. Soc.* 2020, 142, 10267−10272

Read Online

ACCESS | Metrics & More | Article Recommendations | Supporting Information

ABSTRACT: The reaction of *sym*-pentakis(4-aminothiophenyl)corannulene with 2-formyl-6-methylpyridine and Cu^{I} or 2-formyl-1,10-phenanthroline and M^{II} (M = Co, Zn) yields an S_{10}-symmetric 5-fold interlocked [2]catenane of two interpenetrating $[Cu^{I}_{5}L_{2}]^{5+}$ cages or D_5-symmetric $[M^{II}_{5}L_{2}]^{10+}$ cages, respectively. The new structures were characterized by X-ray crystallography, NMR spectroscopy, and mass spectrometry. Density functional theory computations point to dispersive energies on par with traditional covalent bond energies. Subcomponent exchange reactions favored formation of the $[Co^{II}_{5}L_{2}]^{10+}$ cage over the $[Cu^{I}_{10}L_{4}]^{10+}$ catenane. The single cage and catenane each cocrystallized with a corannulene guest to form a bowl-in-bowl substructure.

Despite the intricate and challenging nature of interlocked molecules, knots,[1] ravels,[2] and catenanes[3] of manifold forms have been structurally characterized, including interlocked cages of higher order.[4] A rational synthetic approach for these systems is not yet available, but studies have begun to assess structure−energy relationships for these complexes.[5] In favorable situations, host−guest studies[6] have provided insight into structure−energy correlations of molecular aggregation phenomena more generally.[7] Dispersive interactions become more important with increasing size and can rival covalent bonding energies.[8]

The assembly of subcomponents around metal ion templates[9] yields thermodynamically stable aggregates that may have complex topologies. Judicious choice of subcomponent geometries results in high-symmetry Platonic or Archimedean polyhedra[9a] or even entwined higher-order topological architectures such as links and knots.[10] In this context, corannulene, with 5-fold symmetry, has been the focus of dodecahedral "capsid" construction.[11] Herein, pentafold-substituted corannulene subcomponents capable of generating ligands for tetrahedral Cu^{I} assembled into a surprisingly highly entangled 5-fold interlocked [2]catenane of exceedingly rare S_{10} symmetry.[12] These interlocked [2]catenanes expand the class of interlocked cages from 3-fold[13] and 4-fold[14] to 5-fold structures. A related assembly binding octahedral Zn^{II} or Co^{II} provides a noninterlocked cognate of D_5 symmetry.

Corannulene was chosen as a suitable 5-fold-symmetric scaffold[11,15] because of its potential for functionalization via a variety of synthetic routes[16] and its curved aromatic surface, which may enhance the guest binding properties[17] of assemblies via aromatic stacking interactions.[18] *sym*-Pentakis-(4-aminothiophenyl)corannulene (subcomponent **A**, Figure 1) was synthesized by nucleophilic aromatic substitution from *sym*-pentachlorocorannulene and 4-aminothiophenol in 1,2-dimethylimidazolone in the presence of sodium hydride (Scheme S1).

The reaction of pentaaniline **A** (2 equiv) with 2-formyl-6-methylpyridine (12 equiv) and tetrakis(acetonitrile)copper(I) tetrafluoroborate ($Cu^{I}(MeCN)_4BF_4$) (6 equiv)[19] in CD_3CN at room temperature gave product **1** (Figure 1a). The ^{1}H NMR spectrum of **1** was well-resolved but complex, consisting of two magnetically distinct environments of equal intensity per ligand proton (Figure 2a). All of the peaks between 2.26 and 9.31 ppm displayed a single diffusion constant in the diffusion-ordered ^{1}H NMR (DOSY) spectrum, suggesting that they belonged to a single species.[20]

Crystals of **1** were grown through vapor diffusion of diethyl ether into an acetonitrile solution, and the solid-state structure of **1** was elucidated by single-crystal X-ray diffraction using synchrotron radiation.[21] The crystal structure revealed a $[Cu^{I}_{10}L_{4}]^{10+}$ assembly consisting of a pair of 5-fold interlocked $[Cu^{I}_{5}L_{2}]^{5+}$ cages (Figure 1). The distances of 11.3−11.9 Å between neighboring metal centers create windows of sufficient size to allow two $[Cu^{I}_{5}L_{2}]^{5+}$ cages to interlock to form a [2]catenane. The two ligands within each $[Cu^{I}_{5}L_{2}]^{5+}$ cage display the same handedness, resulting in idealized D_5 cage symmetry. The interlocking of each cage with its enantiomer lends the complete $[Cu^{I}_{10}L_{4}]^{10+}$ assembly S_{10} point-group symmetry.

The two $[Cu^{I}_{5}L_{2}]^{5+}$ cages of the [2]catenane interlock tightly, forming two bowl-in-bowl substructures with stacked corannulenes[18] separated by a distance of 3.69(1) Å. Within a single cage, the distance of 6.93(1) Å between the mean planes of the central pentagons of the corannulenes creates a cavity that matches the form of the intercalated corannulene from the other cage.

The solution NMR data for **1** in CD_3CN are consistent with the solid-state structure, wherein the exo and endo ligands give rise to distinct magnetic environments (Figure 2a). The imine,

Received: March 26, 2020
Published: May 26, 2020

https://dx.doi.org/10.1021/jacs.0c03349
J. Am. Chem. Soc. 2020, 142, 10267−10272

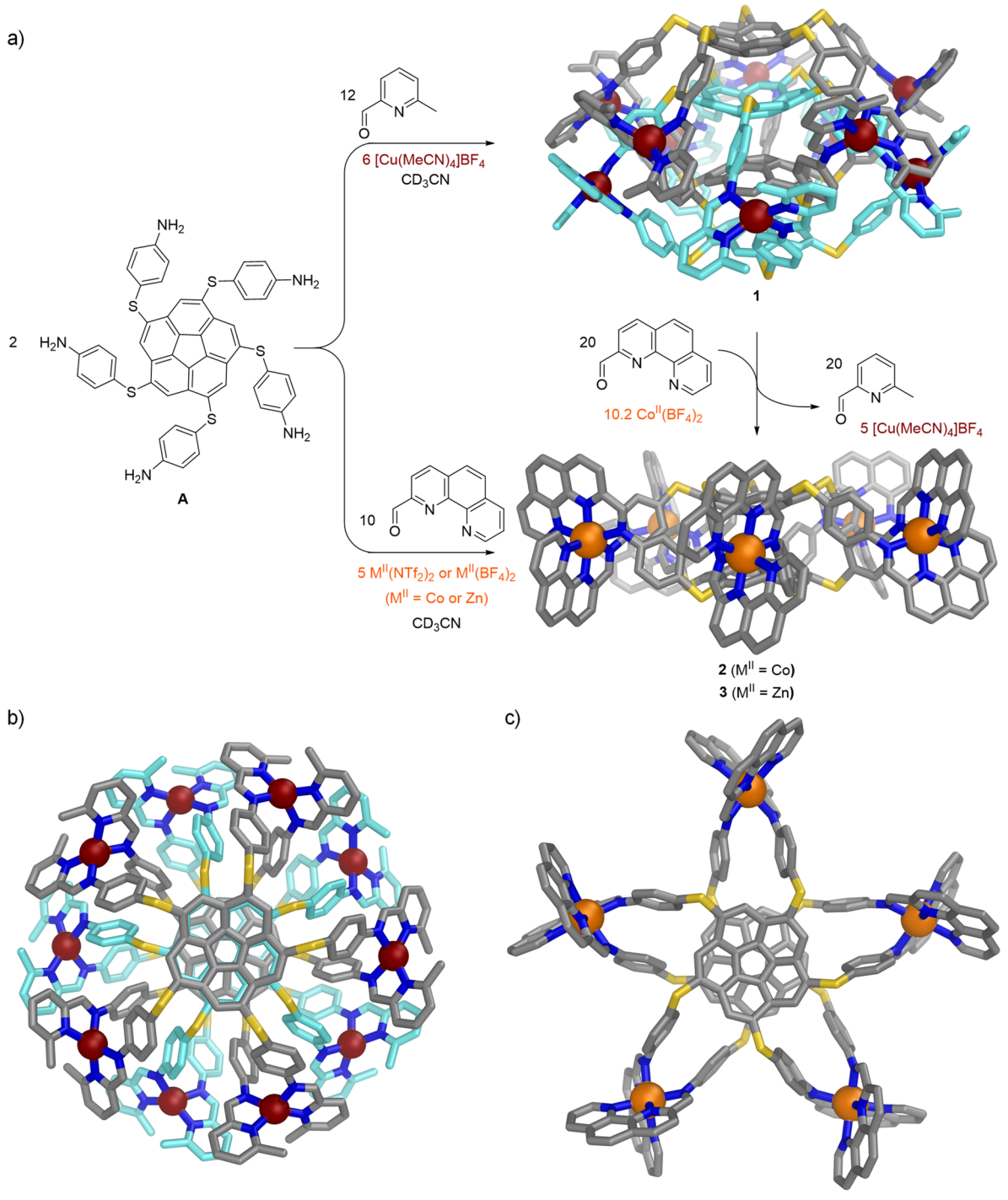

Figure 1. (a) Synthesis of **1**−**3** and the conversion of **1** to **2** through subcomponent exchange. Side-on views of the crystal structures of **1** and **2** are shown. (b) View down the S_{10} axis of the crystal structure of **1**. (c) View down the C_5 axis of the crystal structure of **2**. In the images of **1**, the carbon atoms of the two interlocked $[Cu^{I}_{5}L_2]^{5+}$ cages are colored differently, and only one of the two crystallographically unique assemblies is shown; in all cases hydrogen atoms, counterions, solvent molecules, and disorder have been omitted for clarity.

corannulene, and phenylene signals for the endo ligand are shielded relative to those of the exo ligand. NOE cross-peaks are observed between NMR signals of the two ligands (Figure S8) in a manner consistent with the interlocked structure observed in the solid state. ESI-MS results are also consistent with the $[Cu^{I}_{10}L_4]^{10+}$ composition (Figure 2b).

Density functional theory (DFT) computations of the $[Cu^{I}_{10}L_4]^{10+}$ catenane and the hypothetical $[Cu^{I}_{5}L_2]^{5+}$ cage allowed an assessment of dispersion effects on their relative energetics based on the crystal structure of **1** vs those on the optimized geometry and of the effects of solvation. Neglecting dispersion effects, the energetics of the catenation process in the acetonitrile environment was calculated to be +42.0 kcal/mol (B3LYP/6-31G(d,p)//B3LYP/6-31G(d,p):acetonitrile), indicating that the complex is unbound. With fixed geometry, the energetics including dispersion in the acetonitrile environment is −212 kcal/mol (B3LYP-D3/6-31G(d,p)//B3LYP/6-31G(d,p):acetonitrile). Estimation of the effects of dispersion

https://dx.doi.org/10.1021/jacs.0c03349
J. Am. Chem. Soc. 2020, 142, 10267−10272

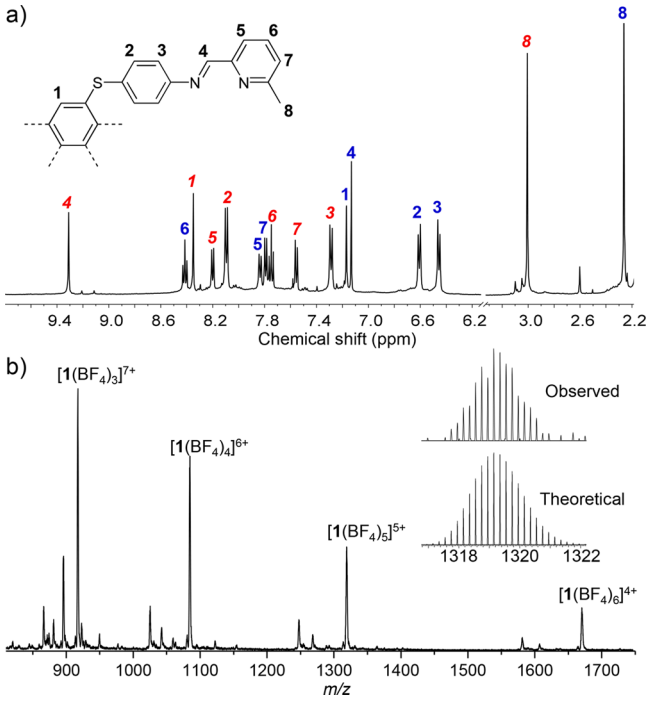

Figure 2. (a) ^{1}H NMR spectra (500 MHz, CD_3CN, 298 K) of **1**. Peak assignments for the interior and exterior ligands are marked with bold blue and italic red labels, respectively. (b) ESI-MS spectrum of **1**. The inset shows the theoretical and observed isotope patterns for the +5 peak.

on the geometry carried out by single-point analysis resulted in a contribution of ~52 kcal/mol. This gives in total ~264 kcal/mol for the catenation process including the effects of dispersion in an acetonitrile environment. Full optimization of the complex including dispersion in the acetonitrile environment (B3LYP-D3/6-31G(d,p):acetonitrile) resulted in a complexation energy of 272.2 kcal/mol, a difference of <8 kcal/mol from the estimated value. This substantial energy contribution for the catenation process is consistent with the large surface area of the corannulene moieties giving rise to substantial van der Waals interactions. Tight packing and the large contact area between ligands within **1** play a central role in driving the selective assembly of this structure.[18,32]

Tridentate donor sites formed from imine condensation with 2-formyl-1,10-phenanthroline, suitable for the octahedral coordination of Co^{II} and Zn^{II},[22] enabled investigation of whether octahedral metal centers also give catenanes incorporating **A**. The reaction of **A** (2 equiv) with 2-formyl-1,10-phenanthroline (10 equiv) and cobalt(II) bis(trifluoromethanesulfonyl)imide ($Co(NTf_2)_2{\cdot}5H_2O$) (5 equiv) in CD_3CN at 353 K yielded **2**. The ^{1}H NMR spectrum reveals a single resonance for each symmetry-equivalent proton, with the signals spread over the range −65.9 to +259.4 ppm as a result of the paramagnetism of Co^{II}.[23] The ESI-MS spectra are consistent with the formula $[Co^{II}_5L_2]^{10+}$ (Figures S14 and S17).

Crystals of **2** (cocrystallized with coronene) were obtained through vapor diffusion of diisopropyl ether into an acetonitrile solution of the BF_4^- salt containing excess coronene.[24] Single-crystal X-ray measurements revealed non-interlocked $[Co^{II}_5L_2]^{10+}$ cages composed of two 5-fold-symmetric ligands of the same handedness bridging five octahedral Co^{II} centers (Figure 1). Both enantiomers of the D_5-symmetric cage are present in the unit cell, related by inversion. The hub pentagon mean planes of the two corannulene moieties sit at a distance of 3.18(1) Å from each other, closer than the 3.2−3.3 Å of graphite planes. The corannulenes in **2** are also flattened compared with those in **1**, with an average bowl depth[25] of 0.84(3) Å versus 0.95(3) and 0.91(1) Å for the exo and endo corannulenes in **1**. Significant distortion from regular octahedral geometry around the metal centers is also observed, with angles of 81−84° between the $Co^{II}N_3$ chelate planes, compared with angles of 84−90° between the $Cu^{I}N_2$ chelate planes in **1**, which displayed a more regular tetrahedral geometry.

Similarly, the reaction of **A** (2 equiv) with 2-formyl-1,10-phenanthroline (10 equiv) and zinc(II) bis(trifluoromethanesulfonyl)imide ($Zn(NTf_2)_2$) (5 equiv) in CD_3CN at 353 K yielded $[Zn^{II}_5L_2]^{10+}$ assembly **3**, as confirmed by ESI-MS. The ^{1}H NMR spectrum also displays a single set of resonances for each ligand proton environment. Crystals were obtained by diffusion of diethyl ether into an acetonitrile solution of **3** containing $CsCB_{11}H_{12}$. Single-crystal X-ray analysis of **3** confirmed it to be isostructural with **2**, although the weakly diffracting nature of the crystals precluded detailed analysis of the structural parameters (Figures S52 and S53).

The relative stabilities of **1** and **2** were probed via subcomponent exchange reactions.[26] A mixture of $Co(BF_4)_2{\cdot}6H_2O$ (10.2 equiv per assembly) and 2-formyl-1,10-phenanthroline (20 equiv per assembly) was added to a solution of **1** in CD_3CN, and the mixture was stirred at 333 K for 24 h and then at 353 K for 72 h. ^{1}H NMR spectra of the reaction mixture showed the disappearance of the diamagnetic signals of **1** followed by the appearance of the paramagnetically shifted signals of **2**. ESI-MS analysis of the resulting mixture indicated the formation of **2** as the major product in solution, indicating its greater stability relative to **1**. We infer that the formation of **2** is enthalpically favored as a consequence of the stronger coordination bonds of the tridentate ligand arms with Co^{II} in **2** relative to the bidentate ligand arms with Cu^{I} in **1** and also entropically favored because one molecule of **1** is converted into two molecules of **2**.

The potential for guests to intercalate[27] within diamagnetic assemblies **1** and **3** or for guests to induce an assembly to rearrange into a suitable host[28] was investigated through the addition of the prospective guests shown in Figure S33. The assemblies were initially investigated as hosts for corannulene, inspired both by the interlocked cage structure of **1** and the observation of corannulene encapsulation inside other polyaromatic hosts[29] and electron-deficient macrocycles.[30] Addition of corannulene (10 equiv) to CD_3CN solutions of **1** or **3** led to shifts in the signals of the ^{1}H NMR spectra of both the host and guest, consistent with fast-exchange complexation on the ^{1}H NMR time scale (Figures S34 and S35).

The host−guest complexes of **1** and **2** with corannulene were also characterized in the solid state through single-crystal X-ray diffraction. Crystals of $(corannulene)_2{\cdot}$**1** were obtained from vapor diffusion of diethyl ether into an acetonitrile solution of **1** saturated with corannulene. The structure reveals two corannulene molecules stacked on the externally facing corannulene moieties of **1** at a distance of 3.71(2) Å (Figure 3a).

Crystals of corannulene·**2** were obtained from vapor diffusion of diethyl ether into an acetonitrile solution of the triflimide salt of **2** saturated with corannulene and containing

https://dx.doi.org/10.1021/jacs.0c03349
J. Am. Chem. Soc. 2020, 142, 10267−10272

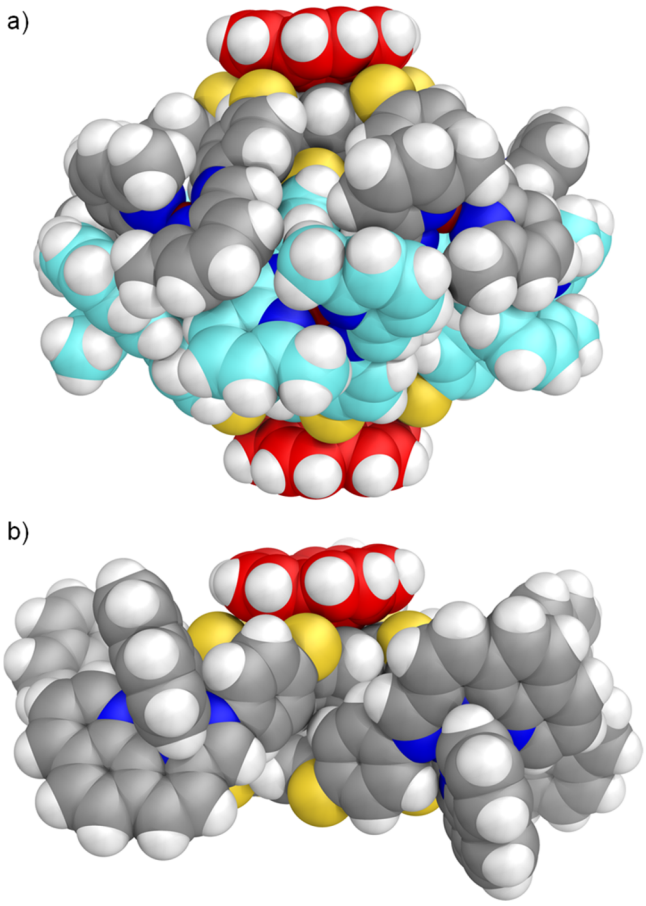

Figure 3. Side views of the cationic parts of the crystal structures of (a) (corannulene)$_2$·**1** and (b) corannulene·**2**. Counterions, solvent molecules, and disorder have been omitted for clarity, and the carbon atoms of the stacked corannulenes are colored red.

excess tetrabutylammonium perrhenate to aid crystallization. In this case only a single corannulene was observed to stack with one of the corannulene moieties of **2**, with a refined occupancy of ca. 0.6 and a distance of 3.57(4) Å between the stacked rings (Figure 3b). The close packing of corannulene on the exterior of **2** in the structure of corannulene·**2** contrasts with that observed in the cocrystal of **2** with coronene (Figures S46 and S47), where the cocrystallized coronene molecules intercalate between ligand arms but do not show any specific stacking interactions with the $[Co^{II}_5L_2]^{10+}$ cation.

The binding mode observed in the solid state is consistent with the solution NMR data, with the largest shifts in host proton signals observed for the *exo*-corannulene protons of **1**, consistent with corannulene undergoing stacking interactions with the exterior of the cage.[22] No interactions were observed between **1** or **3** and planar polycyclic aromatic hydrocarbons,[31] $CB_{11}H_{12}^-$ anions,[32] or spherical C_{60}, despite the known tendency for fullerenes to interact with corannulenes[17] and corannulene-based hosts.[15a,33]

In summary, a 5-fold interlocked $[Cu^{I}_{10}L_4]^{10+}$ [2]catenane, representing a new structure type, has been prepared from Cu^{I} and corannulene-based subcomponent **A**. A DFT study revealed the dominant role of aromatic stacking interactions in driving the formation of the interlocked structure, which is a common feature[13a,d] of other interlocked cage systems. This study demonstrates the power of van der Waals interactions together with coordination-driven assembly to generate new types of highly complex structures.

■ ASSOCIATED CONTENT

Supporting Information

The Supporting Information is available free of charge at https://pubs.acs.org/doi/10.1021/jacs.0c03349.

Detailed descriptions of synthetic procedures, characterization of new compounds, and spectroscopic data (PDF)

X-ray data for **1**·10BF_4 (CCDC 1913638) (CIF)

X-ray data for (corannulene)$_2$·**1**·10BF_4 (CCDC 1913639) (CIF)

X-ray data for **2**·10BF_4 (CCDC 1913641) (CIF)

X-ray data for **2**·coronene·10BF_4 (CCDC 1913642) (CIF)

X-ray data for **2**·10ClO_4 (CCDC 1913643) (CIF)

X-ray data for (corannulene)$_{0.6}$·**2**·4ReO_4·6NTf_2 (CCDC 1913646) (CIF)

X-ray data for **3**·2$CB_{11}H_{12}$·8NTf_2 (CCDC 1913640) (CIF)

■ AUTHOR INFORMATION

Corresponding Authors

Jonathan R. Nitschke − *Department of Chemistry, University of Cambridge, Cambridge CB2 1EW, United Kingdom*; Email: jrn34@cam.ac.uk

Jay S. Siegel − *Health Sciences Platform, Tianjin University, Tianjin 300072, China*; orcid.org/0000-0002-3226-3521; Email: dean_spst@tju.edu.cn

Kim Baldridge − *Health Sciences Platform, Tianjin University, Tianjin 300072, China*; orcid.org/0000-0001-7171-3487; Email: kimbaldridge88@gmail.com

Authors

Tanya K. Ronson − *Department of Chemistry, University of Cambridge, Cambridge CB2 1EW, United Kingdom*; orcid.org/0000-0002-6917-3685

Yujia Wang − *Health Sciences Platform, Tianjin University, Tianjin 300072, China*

Complete contact information is available at: https://pubs.acs.org/10.1021/jacs.0c03349

Notes

The authors declare no competing financial interest.

■ ACKNOWLEDGMENTS

This work was supported by the European Research Council (695009), the U.K. Engineering and Physical Sciences Research Council (EPSRC) (EP/P027067/1), and the National Natural Science Foundation of China (21871207). We thank the EPSRC National Mass Spectrometry Centre (Swansea, U.K.) for high-resolution mass spectrometry and the Diamond Light Source (Didcot, U.K.) for synchrotron beamtime on I19 (MT15768). We thank the National Basic Research Program of China (2015CB856500), the Qian Ren Scholar Program of China, and the Synergetic Innovation Center of Chemical Science and Engineering (Tianjin) for additional support.

https://dx.doi.org/10.1021/jacs.0c03349
J. Am. Chem. Soc. 2020, 142, 10267−10272

REFERENCES

(1) Fielden, S. D. P.; Leigh, D. A.; Woltering, S. L. Molecular Knots. *Angew. Chem., Int. Ed.* **2017**, *56*, 11166.

(2) Li, F.; Clegg, J. K.; Lindoy, L. F.; MacQuart, R. B.; Meehan, G. V. Metallosupramolecular Self-Assembly of a Universal 3-Ravel. *Nat. Commun.* **2011**, *2*, 205.

(3) Ng, A. W. H.; Yee, C.-C.; Au-Yeung, H. Y. Radial Hetero[5]-catenanes: Peripheral Isomer Sequences of the Interlocked Macrocycles. *Angew. Chem., Int. Ed.* **2019**, *58*, 17375.

(4) (a) Zhu, R.; Ding, J.; Jin, L.; Pang, H. Interpenetrated structures appeared in supramolecular cages, MOFs, COFs. *Coord. Chem. Rev.* **2019**, *389*, 119. (b) Frank, M.; Johnstone, M. D.; Clever, G. H. Interpenetrated Cage Structures. *Chem. - Eur. J.* **2016**, *22*, 14104. (c) Zhang, G.; Presly, O.; White, F.; Oppel, I. M.; Mastalerz, M. A Shape-Persistent Quadruply Interlocked Giant Cage Catenane with Two Distinct Pores in the Solid State. *Angew. Chem., Int. Ed.* **2014**, *53*, 5126.

(5) (a) Cougnon, F. B. L.; Au-Yeung, H. Y.; Pantoş, G. D.; Sanders, J. K. M. Exploring the Formation Pathways of Donor−Acceptor Catenanes in Aqueous Dynamic Combinatorial Libraries. *J. Am. Chem. Soc.* **2011**, *133*, 3198. (b) Hasell, T.; Wu, X.; Jones, J. T. A.; Bacsa, J.; Steiner, A.; Mitra, T.; Trewin, A.; Adams, D. J.; Cooper, A. I. Triply interlocked covalent organic cages. *Nat. Chem.* **2010**, *2*, 750. (c) Zhu, K.; Baggi, G.; Loeb, S. J. Ring-through-ring molecular shuttling in a saturated [3]rotaxane. *Nat. Chem.* **2018**, *10*, 625.

(6) (a) Liu, W.; Johnson, A.; Smith, B. D. Guest Back-Folding: A Molecular Design Strategy That Produces a Deep-Red Fluorescent Host/Guest Pair with Picomolar Affinity in Water. *J. Am. Chem. Soc.* **2018**, *140*, 3361. (b) Gropp, C.; Fischer, S.; Husch, T.; Trapp, N.; Carreira, E. M.; Diederich, F. Molecular Recognition and Cocrystallization of Methylated and Halogenated Fragments of Danicalipin A by Enantiopure Alleno-Acetylenic Cage Receptors. *J. Am. Chem. Soc.* **2020**, *142*, 4749. (c) Löffler, S.; Wuttke, A.; Zhang, B.; Holstein, J. J.; Mata, R. A.; Clever, G. H. Influence of size, shape, heteroatom content and dispersive contributions on guest binding in a coordination cage. *Chem. Commun.* **2017**, *53*, 11933.

(7) (a) Turega, S.; Cullen, W.; Whitehead, M.; Hunter, C. A.; Ward, M. D. Mapping the internal recognition surface of an octanuclear coordination cage using guest libraries. *J. Am. Chem. Soc.* **2014**, *136*, 8475. (b) Davis, A. V.; Fiedler, D.; Seeber, G.; Zahl, A.; Van Eldik, R.; Raymond, K. N. Guest Exchange Dynamics in an M_4L_6 Tetrahedral Host. *J. Am. Chem. Soc.* **2006**, *128*, 1324. (c) Jiang, W.; Ajami, D.; Rebek, J. Alkane Lengths Determine Encapsulation Rates and Equilibria. *J. Am. Chem. Soc.* **2012**, *134*, 8070. (d) Qiao, B.; Sengupta, A.; Liu, Y.; McDonald, K. P.; Pink, M.; Anderson, J. R.; Raghavachari, K.; Flood, A. H. Electrostatic and Allosteric Cooperativity in Ion-Pair Binding: A Quantitative and Coupled Experiment−Theory Study with Aryl−Triazole−Ether Macrocycles. *J. Am. Chem. Soc.* **2015**, *137*, 9746.

(8) Toyota, S.; Woods, C. R.; Benaglia, M.; Haldimann, R.; Wärnmark, K.; Hardcastle, K.; Siegel, J. S. Tetranuclear Copper(I)-Biphenanthroline Gridwork: Violation of the Principle of Maximal Donor Coordination Caused by Intercalation and CH-to-N Forces. *Angew. Chem., Int. Ed.* **2001**, *40*, 751.

(9) (a) Ronson, T. K.; Zarra, S.; Black, S. P.; Nitschke, J. R. Metal-organic container molecules through subcomponent self-assembly. *Chem. Commun.* **2013**, *49*, 2476. (b) Zhang, D.; Ronson, T. K.; Nitschke, J. R. Functional Capsules via Subcomponent Self-Assembly. *Acc. Chem. Res.* **2018**, *51*, 2423. (c) Luo, D.; Wang, X.-Z.; Yang, C.; Zhou, X.-P.; Li, D. Self-Assembly of Chiral Metal−Organic Tetartoid. *J. Am. Chem. Soc.* **2018**, *140*, 118. (d) Li, X.; Wu, J.; He, C.; Zhang, R.; Duan, C. Multicomponent self-assembly of a pentanuclear Ir−Zn heterometal−organic polyhedron for carbon dioxide fixation and sulfite sequestration. *Chem. Commun.* **2016**, *52*, 5104.

(10) (a) Bilbeisi, R. A.; Prakasam, T.; Lusi, M.; El Khoury, R.; Platas-Iglesias, C.; Charbonnière, L. J.; Olsen, J.-C.; Elhabiri, M.; Trabolsi, A. [C−H···anion] interactions mediate the templation and anion binding properties of topologically non-trivial metal−organic structures in aqueous solutions. *Chem. Sci.* **2016**, *7*, 2524. (b) Wood, C. S.; Ronson, T. K.; Belenguer, A. M.; Holstein, J. J.; Nitschke, J. R. Two-stage directed self-assembly of a cyclic [3]catenane. *Nat. Chem.* **2015**, *7*, 354. (c) Ayme, J.-F.; Beves, J. E.; Leigh, D. A.; McBurney, R. T.; Rissanen, K.; Schultz, D. A synthetic molecular pentafoil knot. *Nat. Chem.* **2012**, *4*, 15. (d) Chichak, K. S.; Cantrill, S. J.; Pease, A. R.; Chiu, S.-H.; Cave, G. W. V.; Atwood, J. L.; Stoddart, J. F. Molecular Borromean Rings. *Science* **2004**, *304*, 1308.

(11) Chen, Y.-S.; Solel, E.; Huang, Y.-F.; Wang, C.-L.; Tu, T.-H.; Keinan, E.; Chan, Y.-T. Chemical mimicry of viral capsid self-assembly via corannulene-based pentatopic tectons. *Nat. Commun.* **2019**, *10*, 3443.

(12) John, R. P.; Lee, K.; Kim, B. J.; Suh, B. J.; Rhee, H.; Lah, M. S. Modulation of the Ring Size and Nuclearity of Metallamacrocycles via the Steric Effect of Ligands: Preparation and Characterization of 18-Membered Hexanuclear, 24-Membered Octanuclear, and 30-Membered Decanuclear Manganese Metalladiazamacrocycles with α- and β-Branched N-Acylsalicylhydrazides. *Inorg. Chem.* **2005**, *44*, 7109.

(13) (a) Fujita, M.; Fujita, N.; Ogura, K.; Yamaguchi, K. Spontaneous assembly of ten components into two interlocked, identical coordination cages. *Nature* **1999**, *400*, 52. (b) Westcott, A.; Fisher, J.; Harding, L. P.; Rizkallah, P.; Hardie, M. J. Self-assembly of a 3-D triply interlocked chiral [2]catenane. *J. Am. Chem. Soc.* **2008**, *130*, 2950. (c) Henkelis, J. J.; Ronson, T. K.; Harding, L. P.; Hardie, M. J. M_3L_2 metallo-cryptophanes: [2]catenane and simple cages. *Chem. Commun.* **2011**, *47*, 6560. (d) Mishra, A.; Dubey, A.; Min, J. W.; Kim, H.; Stang, P. J.; Chi, K.-W. Molecular self-assembly of arene-Ru based interlocked catenane metalla-cages. *Chem. Commun.* **2014**, *50*, 7542. (e) Yamauchi, Y.; Yoshizawa, M.; Fujita, M. Engineering Stacks of Aromatic Rings by the Interpenetration of Self-Assembled Coordination Cages. *J. Am. Chem. Soc.* **2008**, *130*, 5832. (f) Yang, L.; Jing, X.; An, B.; He, C.; Yang, Y.; Duan, C. Binding of anions in triply interlocked coordination catenanes and dynamic allostery for dehalogenation reactions. *Chem. Sci.* **2018**, *9*, 1050. (g) Li, Y.; Mullen, K. M.; Claridge, T. D. W.; Costa, P. J.; Felix, V.; Beer, P. D. Sulfate anion templated synthesis of a triply interlocked capsule. *Chem. Commun.* **2009**, 7134. (h) Wang, Q.; Yu, C.; Long, H.; Du, Y.; Jin, Y.; Zhang, W. Solution-Phase Dynamic Assembly of Permanently Interlocked Aryleneethynylene Cages through Alkyne Metathesis. *Angew. Chem., Int. Ed.* **2015**, *54*, 7550. (i) Li, H.; Zhang, H.; Lammer, A. D.; Wang, M.; Li, X.; Lynch, V. M.; Sessler, J. L. Quantitative self-assembly of a purely organic three-dimensional catenane in water. *Nat. Chem.* **2015**, *7*, 1003.

(14) (a) Fukuda, M.; Sekiya, R.; Kuroda, R. A Quadruply Stranded Metallohelicate and Its Spontaneous Dimerization into an Interlocked Metallohelicate. *Angew. Chem.* **2008**, *120*, 718. (b) Han, M.; Engelhard, D. M.; Clever, G. H. Self-assembled coordination cages based on banana-shaped ligands. *Chem. Soc. Rev.* **2014**, *43*, 1848.

(15) (a) Sun, W.; Wang, Y.; Ma, L.; Zheng, L.; Fang, W.; Chen, X.; Jiang, H. Self-Assembled Carcerand-like Cage with a Thermoregulated Selective Binding Preference for Purification of High-Purity C_{60} and C_{70}. *J. Org. Chem.* **2018**, *83*, 14667. (b) Huang, F.; Ma, L.; Che, Y.; Jiang, H.; Chen, X.; Wang, Y. Corannulene-Based Coordination Cage with Helical Bias. *J. Org. Chem.* **2018**, *83*, 733.

(16) (a) Pappo, D.; Mejuch, T.; Reany, O.; Solel, E.; Gurram, M.; Keinan, E. Diverse Functionalization of Corannulene: Easy Access to Pentagonal Superstructure. *Org. Lett.* **2009**, *11*, 1063. (b) Nestoros, E.; Stuparu, M. C. Corannulene: a molecular bowl of carbon with multifaceted properties and diverse applications. *Chem. Commun.* **2018**, *54*, 6503. (c) Steinauer, A.; Butterfield, A. M.; Linden, A.; Molina-Ontario, A.; Buck, D. C.; Cotta, R. W.; Echegoyen, L.; Baldridge, K. K.; Siegel, J. S. Tunable Photochemical/Redox Properties of (Phenylthio)ncorannulenes: Application to a Photovoltaic Device. *J. Braz. Chem. Soc.* **2016**, *27*, 1866.

(17) Dawe, L. N.; AlHujran, T. A.; Tran, H.-A.; Mercer, J. I.; Jackson, E. A.; Scott, L. T.; Georghiou, P. E. Corannulene and its penta-tert-butyl derivative co-crystallize 1:1 with pristine C_{60}-fullerene. *Chem. Commun.* **2012**, *48*, 5563.

(18) (a) Dubceac, C.; Sevryugina, Y.; Kuvychko, I. V.; Boltalina, O. V.; Strauss, S. H.; Petrukhina, M. A. Self-Assembly of Aligned Hybrid

https://dx.doi.org/10.1021/jacs.0c03349
J. Am. Chem. Soc. 2020, 142, 10267−10272

One-Dimensional Stacks from Two Complementary π-Bowls. *Cryst. Growth Des.* **2018**, *18*, 307. (b) Haupt, A.; Lentz, D. Tuning the Electron Affinity and Stacking Properties of Corannulene by Introduction of Fluorinated Thioethers. *Chem. - Asian J.* **2018**, *13*, 3022.

(19) Incomplete self-assembly was observed in the absence of excess 2-formyl-6-methylpyridine and $Cu^{I}(MeCN)_4BF_4$.

(20) Peaks for a second, minor species accounting for less than 10% of the signal intensity were also evident in the ^{1}H NMR spectrum of **1**. Those peaks were not intense enough to allow for full NMR characterization. They may correspond to an isomer of **1** with a different stacking pattern having a symmetry too low to be consistent with a single $[Cu^{I}_5L_2]^{5+}$ cage of the type that constitute **1** or to a high-symmetry assembly of such cages.

(21) Allan, D.; Nowell, H.; Barnett, S.; Warren, M.; Wilcox, A.; Christensen, J.; Saunders, L.; Peach, A.; Hooper, M.; Zaja, L.; Patel, S.; Cahill, L.; Marshall, R.; Trimnell, S.; Foster, A.; Bates, T.; Lay, S.; Williams, M.; Hathaway, P.; Winter, G.; Gerstel, M.; Wooley, R. A Novel Dual Air-Bearing Fixed-χ Diffractometer for Small-Molecule Single-Crystal X-ray Diffraction on Beamline I19 at Diamond Light Source. *Crystals* **2017**, *7*, 336.

(22) Rizzuto, F. J.; Wu, W.-Y.; Ronson, T. K.; Nitschke, J. R. Peripheral Templation Generates an $M^{II}_6L_4$ Guest-Binding Capsule. *Angew. Chem., Int. Ed.* **2016**, *55*, 7958.

(23) Hall, B. R.; Manck, L. E.; Tidmarsh, I. S.; Stephenson, A.; Taylor, B. F.; Blaikie, E. J.; Griend, D. A. V.; Ward, M. D. Structures, host-guest chemistry and mechanism of stepwise self-assembly of M_4L_6 tetrahedral cage complexes. *Dalton Trans.* **2011**, *40*, 12132.

(24) X-ray-quality crystals of the pure BF_4^- and ClO_4^- salts of **2** in the absence of coronene were also obtained. However, those data sets showed lower resolution and/or more disorder in the main cation compared with that of the coronene cocrystal that is discussed here in detail. Details of those other data sets can be found in the Supporting Information.

(25) Seiders, T. J.; Baldridge, K. K.; Grube, G. H.; Siegel, J. S. Structure/Energy Correlation of Bowl Depth and Inversion Barrier in Corannulene Derivatives: Combined Experimental and Quantum Mechanical Analysis. *J. Am. Chem. Soc.* **2001**, *123*, 517.

(26) (a) Miller, T. F.; Holloway, L. R.; Nye, P. P.; Lyon, Y.; Beran, G. J. O.; Harman, W. H.; Julian, R. R.; Hooley, R. J. Small Structural Variations Have Large Effects on the Assembly Properties and Spin State of Room Temperature High Spin Fe(II) Iminopyridine Cages. *Inorg. Chem.* **2018**, *57*, 13386. (b) Struch, N.; Topić, F.; Schnakenburg, G.; Rissanen, K.; Lützen, A. Electron-Deficient Pyridylimines: Versatile Building Blocks for Functional Metallosupramolecular Chemistry. *Inorg. Chem.* **2018**, *57*, 241.

(27) Freye, S.; Michel, R.; Stalke, D.; Pawliczek, M.; Frauendorf, H.; Clever, G. H. Template Control over Dimerization and Guest Selectivity of Interpenetrated Coordination Cages. *J. Am. Chem. Soc.* **2013**, *135*, 8476.

(28) (a) Custelcean, R.; Bonnesen, P. V.; Duncan, N. C.; Zhang, X.; Watson, L. A.; Van Berkel, G.; Parson, W. B.; Hay, B. P. Urea-Functionalized M_4L_6 Cage Receptors: Anion-Templated Self-Assembly and Selective Guest Exchange in Aqueous Solutions. *J. Am. Chem. Soc.* **2012**, *134*, 8525. (b) Bai, X.; Jia, C.; Zhao, Y.; Yang, D.; Wang, S.-C.; Li, A.; Chan, Y.-T.; Wang, Y.-Y.; Yang, X.-J.; Wu, B. Peripheral Templation-Modulated Interconversion between an A_4L_6 Tetrahedral Anion Cage and A_2L_3 Triple Helicate with Guest Capture/Release. *Angew. Chem., Int. Ed.* **2018**, *57*, 1851. (c) Kaifer, A. E.; Yi, S.; Brega, V.; Captain, B. Sulfate-templated self-assembly of new M_4L_6 tetrahedral metal organic cages. *Chem. Commun.* **2012**, *48*, 10295. (d) Nakamura, T.; Ube, H.; Miyake, R.; Shionoya, M. A C_{60}-Templated Tetrameric Porphyrin Barrel Complex via Zinc-Mediated Self-Assembly Utilizing Labile Capping Ligands. *J. Am. Chem. Soc.* **2013**, *135*, 18790.

(29) (a) Kishi, N.; Li, Z.; Sei, Y.; Akita, M.; Yoza, K.; Siegel, J. S.; Yoshizawa, M. Wide-Ranging Host Capability of a Pd^{II}-Linked M_2L_4 Molecular Capsule with an Anthracene Shell. *Chem. - Eur. J.* **2013**, *19*, 6313. (b) Schmidt, B. M.; Osuga, T.; Sawada, T.; Hoshino, M.; Fujita, M. Compressed Corannulene in a Molecular Cage. *Angew. Chem., Int. Ed.* **2016**, *55*, 1561. (c) Fan, Q.-J.; Lin, Y.-J.; Hahn, F. E.; Jin, G.-X. Host−guest capability of a three-dimensional heterometallic macrocycle. *Dalton Trans.* **2018**, *47*, 2240.

(30) Juríček, M.; Strutt, N. L.; Barnes, J. C.; Butterfield, A. M.; Dale, E. J.; Baldridge, K. K.; Stoddart, J. F.; Siegel, J. S. Induced-fit catalysis of corannulene bowl-to-bowl inversion. *Nat. Chem.* **2014**, *6*, 222.

(31) In all cases the signals for the hosts appeared at the same or similar chemical shifts (±0.05 ppm) as in the absence of the prospective guest, and the signals for the prospective guest were identical to those in the absence of host, indicating no interaction or the presence of weak nonspecific π-stacking interactions at high guest concentrations.

(32) Although the crystal structure of **3** showed $CB_{11}H_{12}^-$ anions intercalated between the corannulene bowls of neighboring $[Zn^{II}_5L_2]^{10+}$ cages to form 1D stacks (Figure S55), no significant ^{1}H NMR chemical shift changes were observed in solution upon addition of $CsCB_{11}H_{12}$ to CD_3CN solutions of **1** or **3**.

(33) (a) Yang, D.-C.; Li, M.; Chen, C.-F. A bis-corannulene based molecular tweezer with highly sensitive and selective complexation of C_{70} over C_{60}. *Chem. Commun.* **2017**, *53*, 9336. (b) Álvarez, C. M.; García-Escudero, L. A.; García-Rodríguez, R.; Martín-Álvarez, J. M.; Miguel, D.; Rayón, V. M. Enhanced association for C_{70} over C_{60} with a metal complex with corannulene derivate ligands. *Dalton Trans.* **2014**, *43*, 15693. (c) Abeyratne Kuragama, P. L.; Fronczek, F. R.; Sygula, A. Bis-corannulene Receptors for Fullerenes Based on Klärner's Tethers: Reaching the Affinity Limits. *Org. Lett.* **2015**, *17*, 5292.

https://dx.doi.org/10.1021/jacs.0c03349
J. Am. Chem. Soc. 2020, 142, 10267−10272